HHS Public Access

Author manuscript

Arterioscler Thromb Vasc Biol. Author manuscript; available in PMC 2022 January 01.

Published in final edited form as:

Arterioscler Thromb Vasc Biol. 2021 January ; 41(1): 346–359. doi:10.1161/ATVBAHA.120.315472.

Junctional localization of septin 2 is required for organization of junctional proteins in static endothelial monolayers

Joanna Kim, Ph.D.[*], **John A. Cooper, M.D., Ph.D.**[*]

[*]Department of Biochemistry & Molecular Biophysics, Washington University School of Medicine, Saint Louis, MO, USA.

Abstract

Objective: Septin 2 is enriched at junctions in human microvascular endothelial monolayers. The junctional localization of septin 2 is necessary for organization of cell-cell adhesion proteins of endothelial cells.

Approach and Results: Septin 2 was depleted at jucntions by suppression of expression using shRNA, treatment with inflammatory cytokine, TNF-α, and ectopic overexpression of septin 2 PIP_2 binding mutant (BM) defect in interaction with plasma membrane. Under those conditions, organizations and expression levels of various junctional proteins were analysed. Confocal images of immunofluorescence staining showed substantial disorganization of adherens junctional proteins, nectin-2 and afadin, tight junction protein, ZO-1, and intercellular adhesion protein, PECAM-1. Immunoblots for those proteins did not show significant changes in expression except for nectin-2 that highly increased in expression. Signifcant differential gene expression profiles and biological pathway analysis by septin 2 suppression and by TNF-α treatment using RNAseq showed common overlapping pathways. The commonalities in expression may be consistent with the similar effects on the overall organization of cell-cell adhesion proteins.

Conclusions: Localization of septin 2 at cell junctions are required for the arrangement of junctional proteins and the integrity of the barrier formed by endothelial monolayers.

Graphical Abstract

Corresponding author: John A. Cooper, Campus Box 8231, 660 S. Euclid Ave., Saint Louis, MO 63110-1093, jcooper11@gmail.com, Phone: (314) 362-3964, Fax: (314) 362-7183.

Competing interests

The authors report no conflicts of Interest

Data availability

Raw data for RNA-Seq experiments is available from the authors by direct request and via the GEO dataset repository at NCBI (https://www.ncbi.nlm.nih.gov/geo).

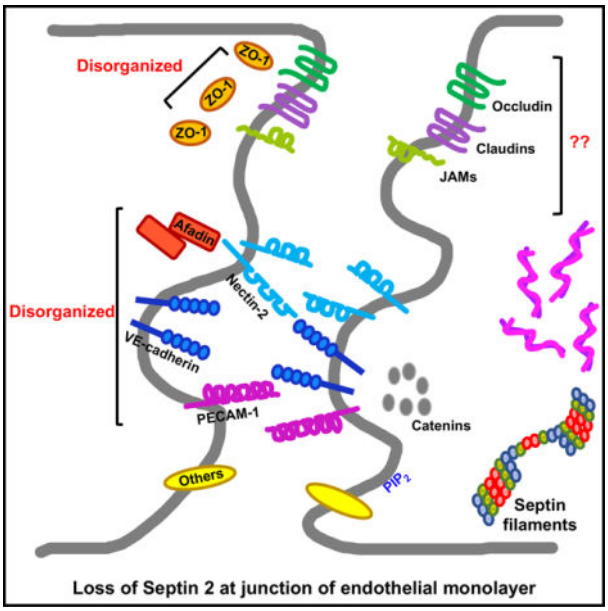

Introduction

The septin family of genes and proteins were discovered as cytoskeletal elements important for cell division in budding yeast[1]. Septins form filaments that assemble into a ring associated with the cell membrane at the site of cytokinesis[2,3]. Septins are found in a wide variety of eukaryotes and cell types, where they play a diverse set of roles in cellular processes[4–6]. Septin family proteins are well-conserved across species, and mammalian septins consist of 13 members classified into 4 different groups on the basis of sequence similarity and domain structure[7–9].

Septin family proteins form homo-and hetero-oligomers *in vitro* and *in vivo*[10,11]. The oligomers assemble into filaments and associate with membranes via a polybasic domain[12–14], and the filaments assemble further into ring- and gauze-shaped higher-order arrays *in vitro* and in cells[3,15,16]. Thus, septin filaments represent an important element of the membrane cytoskeleton, and they contribute to membrane-associated cellular functions[10,11,17]. For instance, septin filaments are enriched at positively curved areas of plasma membrane, providing interactive feedback between cell shape and the cytoskeleton[10,18–20]. In addition, septins play roles in intracellular membrane-associated processes[21–23], such as mitochondrial fission[24] and endomembrane fusion[25]. Septin filaments interact with other cytoskeletal elements, including actin filaments and microtubules, providing crosstalk regulation of cell morphology, migration, and other functions in cooperative manners in multiple cell settings[26–31].

The endothelial monolayer is a continuous thin layer of endothelial cells that lines the interior surface of blood and lymphatic vessels. The endothelial monolayer is an active and regulated barrier[32], playing crucial roles in multiple biological processes, including vascular tone, thrombosis / thrombolysis, cell adhesion and passage of small molecules and cells. In order to perform these diverse roles, maintenance and regulation of the barrier structure and

monolayer integrity are crucial[33–35]. Endothelial cell-cell junctions are key components in regulating the integrity of the endothelial monolayer, and they consist of adherens junctions, tight junctions, and gap junctions, along with other diffusely localized cell adhesion proteins[36–38].

Adherens junctions contain vascular endothelial cadherin (VE-cadherin), nectin, and afadin. VE-cadherin, the dominant component of adherens junctions, is a transmembrane glycoprotein that forms homodimers via its extracellular domain. The cytosolic domain of VE-cadherin interacts with catenin complexes (p120, β-catenin, and α-catenin) linking actin filaments to the junctions[39]. Afadin interacts with actin filaments and nectin as part of its recruitment to VE-cadherin-based adherens junctions[40]. Afadin is also recruited to tight junctions[40,41], the closely apposed junctional areas assembled by intercellular adhesion molecules including claudins, occludin, and zonula occludens (ZOs)[42,43]. ZO proteins function as cytosolic scaffolds that directly bind to actin filaments and are recruited to lateral membranes, where they bind claudins and occludin to promote tight junction assembly[44]. Like afadin, ZO proteins have shared functions to promote the assembly of both tight junction and adherens junction[45]. Junctional adhesion molecules (JAMs) are another set of intercellular adhesion components that are located at tight junctions and regulate interactions between endothelial cells and between leukocytes and endothelial cells[46]. Gap junctions are comprised of members of the connexin protein family. Connexon (hexameric connexin complex) form channel-like structure between adjacent cells and regulate transferring intracellular molecules[47,48]. In addition to these molecules, platelet endothelial cell adhesion molecule (PECAM-1, also known as CD31)[49] and MIC-2 (also known as CD99) are recruited to endothelial cell junctions, where they regulate transmigration of leukocytes across the junctions[50,51].

Cell junctions are supported in the cytoplasm by elements of the cytoskeleton associated with the plasma membrane, notably actin filaments (F-actin)[52–56]. In previous work, we characterized septin filaments as a membrane cytoskeleton component of endothelial cells. Septins were found at positively curved membrane areas, near the base of actin-based lamellipodial protrusions. Loss of septins impaired the assembly and function of VE-cadherin-based adherens junctions and the overall integrity of endothelial monolayers[20]. Here, we investigated whether and how septins influence the integrity of other cell junctional molecules, using the same endothelial cell monolayer system. We also investigated the mechanism of septin association with the membrane and the relationship of septin function to effects of the inflammatory mediator TNF-α on endothelial junctional integrity.

Materials and Methods

The data that support the findings of this study are available from the corresponding author upon request. The RNA-Seq data files are available from GEO dataset repository at NCBI (https://www.ncbi.nlm.nih.gov/geo).

Cells and Cell Culture

Primary human dermal microvascular endothelial cells (HDMVECs) were cultured as described[20]. In brief, primary human dermal microvascular endothelial cells (HDMVECs)

from neonates, obtained from Lonza Bioscience (Walkersville, MD, USA), were grown in EGM-2MV (Microvascular Endothelial Cell Growth Medium-2) medium from Lonza Bioscience. HDMVECs were used between passages 3 and 8 for experiments. For fluorescence imaging, 5×10^4 HDMVECs were seeded into 14-mm glass-bottom dishes (MatTek Corporation, Ashland, MA, USA) and cultured for two to three days until cells formed continuous monolayers. For infection of cells with lentivirus, 2×10^5 cells were seeded into 6-well plates, cultured for one day, and infected with lentiviruses in culture media containing 10 μg/mL protamine sulfate. At one day post-infection, media was replaced with fresh culture media and cells were incubated for two to three additional days to suppress protein expression or to overexpress protein.

Lentivirus production was performed as described[20]. In brief, HEK293T cells were grown in Dulbecco's modified eagle's medium (DMEM) (Gibco Thermo Fisher Scientific, Gaithersburg, MD, USA) containing 10% FBS (Hyclone, GE healthcare Life Technology, South Logan, UT, USA) and 1% streptomycin/penicillin (Gibco Thermo Fisher Scientific, Gaithersburg, MD, USA). For lentivirus production, HEK293T cells in 150-mm dishes (Corning Falcon ®, NY, USA) were transfected with 3rd generation lentivirus packaging plasmids, pMDLg/pRRE, pRSV-Rev, and pMD2.G, using TransIT-LT1 transfection reagent (MirusBio, Wisconsin, USA) and incubated for one day, followed by two days of incubation with high serum (30% FBS)-containing DMEM. Lentivirus supernatant was filtered with a 0.45-μm pore filter (EMD Millipore Corp, USA) and concentrated at 20,000 rpm for 2 hrs. Lentiviruses were resuspended in 1 mL in high serum (30% FBS)-containing DMEM and stored at −70°C. To suppress protein expression, HDMVECs grown in 6-well plates were infected with 60 μL of lentiviruses and incubated for 3–4 days, leading to >80% suppression of protein. For overexpression of transgenes, HDMVECs cultured in 6-well plates were infected with 100–200 μL of lentivirus and incubated for 3–4 days. Suppression and overexpression of protein were confirmed with immunoblot or immunofluorescence staining.

Antibodies and Reagents

Mouse monoclonal anti-human VE-cadherin antibody (clone 55–7H1), polyclonal rabbit anti-human septin 2 (Atlas Antibodies, Cat. # HPA018481), mouse monoclonal anti-human GAPDH (clone 6C5), mouse monoclonal anti-GFP antibody (9F9.F9) were obtained and used as described[20]. Anti-human nectin-2 antibody (Cat.# AF2229) and anti-human afadin antibody (clone 851204) were obtained from R & D Systems (Minneapolis, MN, USA). Anti-human PECAM-1 antibody (JC/70A) was obtained from Abcam (Cat.# ab9498) (Cambridge, MA, USA) and anti-human ZO-1 antibody was obtained from Invitrogen ThermoFisher (Carlsbad, CA, USA). Donkey anti-goat IgG H&L Alexa Fluor® 568 (Cat.# ab175704), donkey anti-rabbit IgG H&L Alexa Fluor® 488 (Cat.# ab150073), and donkey anti-mouse H&L Alexa Fluor® 488 (Cat.# ab150105) were obtained from Abcam (Cambridge, MA, USA). Phalloidin conjugated with Alexa Fluor™−647 and secondary antibodies conjugated with horseradish peroxidase were obtained from Molecular Probes ThermoFisher (Eugene, OR, USA) and Sigma-Aldrich (St Louis, MO, USA), respectively.

Reagents and buffers

Tumor necrosis factor alpha (TNF-) was obtained from Gibco ThermoFisher (Gaithersburg, MD, USA), and fibronectin was obtained from Sigma-Aldrich (St Louis, MO, USA). ProLong Gold anti-fade solution was obtained from Molecular Probes ThermoFisher (Eugene, OR, USA). T4 DNA Ligase were obtained from Invitrogen ThermoFisher (Carlsbad, CA, USA). PfuTurbo DNA polymerase and QuikChange Site-Directed Mutagenesis Kit were obtained from Agilent Technologies (Santa Clara, CA, USA).

Plasmids expressing two shRNA oligonucleotides targeting septin 2 and one shRNA oligonucleotide targeting LacZ, to serve as a control, were obtained and used as described[20].

Site-directed mutagenesis and Cloning

To create septin 2 PIP_2 binding mutant (PIP_2BM), we changed arginine (R) and lysine (K) residues at positions 29 and 30 and lysine residues at positions 33 and 34 to alanine (A) using the QuikChange Site-directed Mutagenesis Kit (Agilent Technologies) according to the manufacturer's protocol. pBOB-septin 2 wt-GFP[20] was used as a template for PCR-amplified mutagenesis with primers containing multiple mutation sites. Lentivirus for expression of septin 2 PIP_2BM -GFP was produced as described[20].

Immunofluorescence staining

HDMVEC monolayers were fixed by adding an equal volume of 2X fixation solution composed of freshly dissolved 5% paraformaldehyde in PIPES buffer, prewarmed to 37°C[57], directly into culture dishes and incubating at 37°C for 10 min. After removing the fixation solution, cell samples were permeabilized by incubation in 0.1% Triton X-100 in PBS at RT for 5 min. Samples were washed with PBS three times, incubated in blocking buffer (3% BSA in PBS) for at least 30 min, followed by primary antibodies at 4°C overnight, and secondary antibodies conjugated with Alexa fluorescent dyes at RT for 1 hr. Antibodies were diluted in blocking buffer. Samples were washed with PBS three times after primary and secondary antibody incubations. For phalloidin staining, fluorescent phalloidin was added to the secondary antibody solution. Samples were mounted with ProLong Gold anti-fade reagent.

Fluorescence images were collection with a Nikon A1R resonant scanning confocal system using a 40x objective. Z-stacks were collected with a 0.25 μm step size. Images are presented as 2-D projections of Z-stacks prepared with the Fiji implementation of ImageJ open-source software (https://fiji.sc/)[58].

Measurement of cell area

To measure cell area, we counted the total numbers of cells in fluorescently stained confocal images of control and septin 2-suppressed HDMVECs. Average cell size was calculated by dividing the area of the entire image by the total cell number.

Blind scoring of junctional molecule organization

To quantify the organization of junctional molecules, each confocal image was assigned a random number. Each junction in each image was defined from one end to the other, and

each junction was assigned a number. Junctions shorter than a cell nucleus were excluded from the scoring process. Blinded volunteer observers in our laboratory group scored the organization of nectin-2, afadin and ZO-1, based on a set of defined criteria. Scores from 1 to 4 were assigned, and the defined criteria are listed in Supplemental Table 1. For PECAM-1, a similar process was employed, and the scoring system extended only from 1 to 3 due to the character of the PECAM-1 staining distribution. PECAM-1 score definitions were as follows: 1, one continuous solid line; score 2, partial disruptions affecting up to 70% of the length of a junction; score 3, severe and / or multiple disruptions across the entire length of a junction or complete absence of a junctional pattern. Scores were tabulated in Excel and then transferred to GraphPad Prism for statistical analysis and plots.

Cell viability assay

HDMVECs (2×10^4 cells) were grown in 24 well plates and infected with lentiviruses carrying shControl and shSeptin 2. Cell viability was assayed using a Bimake Cell counting Kit-8 (Bimake.com, TX, USA), according to the manufacturer's protocol. Cells were incubated with the CCK-8 reagent for 2 hrs, at various time points after infection with lentivirus and the absorbance was read by Cytation 5 Cell Imaging Multi-Mode Reader (BioTek Instruments Inc., Vermont, USA).

Immunoblots

HDMVECs were washed with RT PBS and lysed by adding 1X SDS-PAGE loading buffer into culture dishes. These whole-cell lysates (WCLs) were harvested by scraping the dish and boiling the sample in a heating block for 10 min. WCLs were loaded onto 4–20% gradient SDS polyacrylamide gels, separated by electrophoresis, and transferred to PVDF membrane (MilliporeSigma Corp., St Louis, MO, USA) at 90 V for 1 hr at 4°C. The membrane was incubated in blocking buffer (4% BSA in Tris-buffered saline, 0.1% Tween 20 (TBST) buffer) at RT for 30 min and in a primary antibody mixture at 4°C overnight. After washing with PBS with 5 times, the membrane was incubated in horseradish-peroxidase-conjugated secondary antibodies at RT for 1 hr. The membrane was incubated with enhanced chemiluminescence solution at RT for 5 min and developed for autoradiography.

RNA Sequencing

HDMVECs were grown to confluence in 100-mm dishes, treated in various ways, and total RNA was prepared using an RNeasy mini kit (Qiagen, Germantown, MD, USA) according to manufacturer protocol. Samples were indexed, pooled, and sequenced on an Illumina HiSeq system by the Genome Technology Access Center (GTAC) of Washington University School of Medicine. Base calls and demultiplexing were performed with Illumina's bcl2fastq software and a custom python demultiplexing program with a maximum of one mismatch in the indexing read. RNA-Seq reads were then aligned to the human Ensembl release 76 primary assembly with STAR version 2.5.1a[59]. Gene counts were derived from the number of uniquely aligned unambiguous reads by Subread:featureCount version 1.4.6-p5[60]. Isoform expression of known Ensembl transcripts were estimated with Salmon version 0.8.2[61]. Sequencing quality performance was assessed based on total number of aligned reads, total number of uniquely aligned reads, and detected features. The ribosomal fraction,

known junction saturation, and read distribution over known gene models were quantified with RSeQC version 2.6.2[62].

Gene counts were imported into the R/Bioconductor package EdgeR[63], and TMM normalization size factors were calculated to adjust for differences in library size among samples. Ribosomal genes and genes not expressed in the smallest group size minus one sample greater than one count-per-million were excluded from further analysis. The TMM size factors and the matrix of counts were imported into the R/Bioconductor package Limma[64]. Weighted likelihoods based on the observed mean-variance relationship of every gene and sample were calculated for all samples with the application voomWithQualityWeights[65]. The performance of all genes was assessed with plots of the residual standard deviation of every gene to their average log-count with a robustly fitted trend line of the residuals. Differential expression analysis was performed to analyze for differences between conditions, and the results were filtered to include only genes with Benjamini-Hochberg false-discovery rate adjusted p-values ≤ 0.05.

Gene counts were imported into Partek Flow software (Partek® Flow®, Version 8.0, 2020, Partek Inc., St Louis, MO) in the format of general workflows to be used for principle component analysis (PCA), gene ontology (GO) terms by p-values and log fold-changes.

Statistical analysis

We used GraphPad Prism v8.4.3 (www.graphpad.com) to perform statistical analyses. To calculate significance for blinded scores of junction morphology, comparing control versus test samples, we added the values of the scores from each observer for each set of experiments, and we performed Chi-squared analysis in Prism. We tested for statistical significance among observers using 2-way ANOVA and multiple comparison analysis. No observer differed from any other observer to a statistically significant extent.

Results

We reported previously that septins were required for the proper organization of VE-cadherin at cell junctions of microvascular endothelial monolayers composed of human primary endothelial cells by observing that loss of septin 2 disrupted VE-cadherin structure, membrane dynamics, and junctional integrity[20]. The junctional integrity of the endothelial monolayer is tightly regulated by a number of diverse intercellular adhesion proteins at cell-cell contact sites in response to cellular and molecular stimuli[66]. In this study, we extended our analysis by asking whether septin 2 is required to regulate the organization of other adhesion and junctional proteins, including nectin-2, afadin, PECAM-1, and ZO-1.

We localized these junctional proteins in endothelial monolayers of primary human dermal microvascular cells (HDMVECs) in which septin 2 was depleted by shRNA expression (Suppression levels and cell viability are in Supplemental Fig.1). Figure 1 shows immunofluorescence staining for endogenous septin 2 (green), intercellular adhesion proteins (red), and actin filaments, in response to septin 2 suppression. In control cells, nectin-2 (Fig. 1A, upper panels, with inset) and afadin (Fig. 1B, upper panels, with inset) are arranged as continuous solid-line structures running parallel to cell-cell junction with or

without local ruffles at cell junctions (yellow arrows in insets). In septin 2-suppressed cells, the organization of the junctional proteins changed substantially, to a pattern that was discontinuous, broader and perpendicular to cell-cell junction (Fig. 1A and B. Lower panels). The organization of PECAM-1 (Fig. 1C) also showed dramatic changes, similar to those for nectin-2 and afadin, upon depletion of septin 2. In addition, we examined the effect of septin 2 suppression on a tight junction component, ZO-1 (Fig.1D). ZO-1 also displayed a disorganized arrangement in septin 2-suppressed cells (Fig.1D, lower panels, with inset).

Quantitative analysis of the organization of nectin-2, afadin, PECAM-1, and ZO-1 in control and septin 2-suppressed HDMVECs was performed by a set of several blinded observers using a system of scoring criteria defined in advance (see Methods and Supplemental Table 1). Comparing control with septin 2-suppressed samples, the results were highly statistically significant (Chi-squared analysis, p-value < 0.0001), and variances among observers were not statistically significant. Septin 2 suppression caused disorganization of all of these various intercellular junctional components of microvascular endothelial cells.

Next, we asked whether the inflammatory mediator TNF-α would elicit disorganization of the same junctional proteins. In previous work, we found that septin 2 filaments, normally enriched at cell junctions, were depleted from these regions and accumulated in the cytoplasm, in response to TNF-α treatment. VE-cadherin organization was also disrupted, in a manner similar to that of septin 2 depletion[20]. Here, we examined the effect of TNF-α treatment on the arrangement of other intercellular adhesion proteins (Fig. 2 and Supplemental Fig. 2 for lower TNF-α). Control untreated HDMVEC monolayers showed continuous thin-line arrangement running parallel to cell-cell junction with or without local ruffles for all the adhesion proteins (Fig. 2, A–D, upper panels with insets). TNF-α treated cells showed dramatically altered and disorganized arrangements for nectin-2, afadin, PECAM-1, and ZO-1 (Fig. 2, A–D, lower panels, with insets). The organization of nectin-2, afadin, PECAM-1, and ZO-1 in untreated and TNF-α treated HDMVECs were scored by blinded observers and quantified as in Figure 1. Differences in control samples versus TNF-α treated samples were statistically significant (Chi-squared analysis, p-value < 0.0001) and variances among observers were statistically not significant. In addition, TNF-α treatment led to loss of septin 2 from near cell junctions with accumulation in the cytoplasm (Fig. 2).

Analysis of Protein and Gene Expression

We considered the possibility that the effects of septin 2 suppression and TNF-α treatment might result from changes in the level of expression junction-associated proteins. In particular, we reasoned that cooperative assembly of filaments and macromolecular complexes might be affected in a non-linear manner by decreases in levels of individual protein components. We examined expression levels in two ways - by protein immunoblots with specific antibodies (Fig. 3) and by RNA-Seq analysis of whole-cell RNA samples (Fig. 4). Immunoblot analysis revealed that nectin-2 protein level was increased in response to septin 2 suppression (Fig. 3A) and TNF-α treatment (Fig. 3B). The protein levels of afadin, PECAM-1, and ZO-1 did not change significantly with either septin 2 depletion (Fig. 3A) or with TNF-α treatment (Fig. 3B). As noted above, the effects of septin 2 suppression and TNF-α treatment were similar to each other.

RNA-Seq results and analyses are presented in Figure 4 and Supplemental Tables 2–5. Principal component analysis (PCA) was performed with all genes represented (Fig. 4A). Volcano plots highlight differential gene expression profiles in response to septin 2 suppression and TNF-α treatment using log 2 fold change over 2 (Fig. 5, B and C). In addition, top-ranked genes with significant differential changes were revealed for both experimental conditions. For septin 2 suppression, ADAM9, ACER2, CYGB, and ENKUR were most-strongly upregulated, while FLN4, ENTPD5, PCDDH10, NDRG4, COL1A2, and CNR1 were decreased (Fig. 4B). Treatment with TNF-α led to significant changes in a different set of genes, with strongest up-regulation for U2AF1, CXCL11, BEST1, and SPARCL1, and strongest down-regulation for SPATA13, FAAH, CCL1, WHRN, FOXF1, and PHOD3 (Fig. 4C). Lists of genes with > 2-fold changes in expression in response to septin 2 suppression and TNF- α treatment are listed in Supplemental Tables 2 and 3.

We looked specifically at RNA levels for genes encoding the junctional proteins examined above, namely VE-cadherin (CDH5), nectin-2 (NECTIN2), afadin (AFND), PECAM-1 (PECAM1), and ZO-1 (TJP1). VE-cadherin (CDH5) RNA levels were significantly increased by septin 2 suppression and slightly increased by TNF-α treatment (Fig. 4B and C, pink), consistent with the protein expression analysis by immunoblot in our previous study[20]. We observed no significant changes in expression for nectin-2, afadin, PECAM-1, or ZO-1 (Fig. 4B and C, pink, Supplemental Tables 4 and 5).

We also analyzed the data with respect to biological systems using Gene Ontology terms, KEGG pathways (data not shown) and Heatmaps (data not shown). The Top-ranked GO terms by p-values and $\log_2$ fold change, and the GO terms for cell adhesion, in septin 2 suppression and TNF-α treatment were revealed; they are listed in Figure 4, panels D to I. GO terms in the top tier of p-values included ones for chromosome segregation and DNA repair in septin 2 suppression (Fig. 4D). Impairments in these processes may be expected to slow the cell cycle, and that appears to be consistent with the finding of an increase in cell size, by 1.5 fold, with septin 2 suppression (Supplemental Table 6). For TNF-α treatment, GO terms related to immune system function were in the top tier, as one might expect (Fig. 4E). Analysis of GO terms based on $\log_2$ fold changes revealed a variety of biological systems in both conditions (Fig. 4F and G). Of note, GO terms related to cell adhesion were revealed in the GO term analysis based on p-values, in both cases - septin 2 suppression and TNF-α treatment.

Taken together, the differential gene expression profiles and the gene ontology term analysis of the RNA sequence results revealed a number of overlapping pathways in common for septin 2 suppression and TNF-α treatment. The commonalities in expression may be consistent with the common effects on the overall organization of cell-cell adhesion proteins and cell junctions.

Polybasic Domain of Septin 2 and Membrane Localization

As described above, TNF-α treatment led to loss of septin 2 from near cell junctions, with accumulation in the cytoplasm (Fig. 2), and we previously observed septin 2 accumulated at regions of positive membrane curvature. We hypothesized that septin 2 localizes to the plasma membrane in our cells via an association of its polybasic domain with acidic

phospholipids, because arginine and lysine residues in the polybasic domain of human septins are important for binding to PIP_2 and PIP_3 *in vitro* and in cells, and because these basic residues are conserved in the polybasic domain of septin 2[12,13,67–69]. To test this hypothesis, we asked whether point mutations of the basic residues in the polybasic domain of septin 2 would disrupt septin 2 accumulation and organization of endothelial cell junction proteins. We changed four arginine (R) and lysine (K) residues to alanine (A) in the poly basic domain at the N-terminal region of septin 2 (diagrammed in Fig. 5A) to create a PIP_2-binding defective form of septin 2, which we refer to as "septin 2 PIP_2BM".

We expressed septin 2 PIP_2BM in HDMVECs using a pBOB-GFP lentiviral expression system (Fig. 5B), and we examined cells by immunofluorescence, using antibodies to GFP and to septin 2 (Supplemental Fig. 3). Septin 2 wild-type (wt)-GFP was expressed as a control. For septin 2 wt-GFP, the anti-GFP staining localized to cell junctions as expected (Supplemental Fig. 3A, cells with blue pentagons), and anti-septin 2 staining, reflecting the distribution of expressed and endogenous septin 2, also localized to cell junctions (cells with blue pentagons versus cells will magenta dots) as usual. In contrast, septin 2 PIP_2BM-GFP expressed in cells failed to localize to cell junctions, supporting our hypothesis that the basic residues mediate interaction of septin 2 with the membrane. Moreover, expression of septin 2 PIP_2BM-GFP produced a dominant negative effect; endogenous septin 2 was lost from junctional localizations, with accumulation in the cytoplasm, based on anti-septin 2 staining (Supplemental Fig. 3B, inset. Infected cells are labeled with blue pentagons, and uninfected cells are labeled with magenta dots). Thus, septin 2 PIP_2BM did not localize to the plasma membrane, and it had a dominant negative effect on the localization of endogenous septin 2, consistent with the hetero-oligomeric and filamentous nature of septins in cells.

We asked whether expression of septin 2 PIP_2BM affected the arrangement and organization of other endothelial junctional proteins, by immunofluorescence. Nectin-2 and afadin are shown in Figure 5, C and D, as representative examples of junctional proteins. Septin 2 wt expression did not affect the continuous thin-line arrangement of nectin-2 (Fig. 5C, upper panels, with inset) and afadin (Fig. 5D, upper panels, with inset) at cell junctions. In contrast, overexpression of septin 2 PIP_2BM disrupted the organization of nectin-2 (Fig. 5C, lower panels, with inset) and afadin (Fig. 5C, lower panels, with inset) at cell junctions. The disruption pattern was similar to those produced by septin 2 suppression and by TNF-α treatment illustrated above (Figs. 1 and 2). We conclude that septin 2 tethers directly to the plasma membrane via interaction of arginine and lysine residues in the polybasic domain of septin 2 with anionic phosphoinositides of plasma membrane, and that this interaction is required for the proper organization and integrity of cell junctions.

Discussion

Endothelial Cell Junction Components and Septins

In this study, we discovered that junctional localization of septin 2 is required to preserve the proper organization of a number of cell junctional proteins of microvascular endothelial cell monolayers. We focused on the adherens junction proteins, nectin-2 and afadin, the tight junction protein ZO-1, and the general adhesion protein PECAM-1, extending our previous

study of VE-cadherin[20]. We found striking disorganization of all these junctional proteins in response to depletion of septin 2 protein.

We considered that the loss of organization of the junctional proteins might result from decreased expression levels of the proteins, especially if their assembly involved positive cooperativity and multicomponent oligomerization. However, we found that the protein levels of afadin, PECAM-1, and ZO-1 did not change, and the level of nectin-2 protein increased. Thus, the disruption of their junctional organization was not due simply to decreased levels of proteins. These results are similar to and consistent with those observed for VE-cadherin in our previous study[20]. We also examined gene expression levels, based on analysis of RNA by RNA-Seq, and those results were consistent with the results from assays of protein.

The most likely role for septins in the organization of these various junctional components, in our view, is to support the positively curved regions of membrane at the base of actin-based lamellipodial protrusions, which was the conclusion of our previous study[20]. Endothelial cells appear to be constantly forming protrusions that push toward each other to form adhesions, as indicated by previous studies[54,55], most notably that of Efimova and Svitkina[70]. The accumulated evidence supports a model in which sites of cell-cell contact, where membrane protrusions from apposing cells meet, are locations where adhesive junctional cell surface molecules interact with their counterparts on adjacent cells and assemble into the supramolecular structures defined as cell junctions.

The junctional components that we examined included ones found in endothelial cell adherens junctions, in tight junctions and diffusely located on the surface. Adherens junctions of endothelial cells contain VE-cadherin, nectin-2, and afadin[71]. Nectin-2 and afadin are recruited to VE-cadherin-containing adherens junctions in both epithelial cells[72] and endothelial cells[73]. PECAM-1 is localized at intercellular adhesion sites between endothelial cells and is also found at contacts between endothelial cells and platelets[74]. Tight junctions of endothelial cells include the protein Zona Occludens-1 (ZO-1).

Septin - Membrane Interactions

Septin proteins and filaments are known to interact directly with membrane lipids[13,67–69,75], accumulating at locations with positive curvature[18,76,77]. This direct interaction can be mediated by a polybasic region of septins interacting with acidic head groups of phospholipids on the membrane surface[78]. To investigate whether an electrostatic interaction mechanism might also account for the association of septins with plasma membranes in endothelial cells, we tested the effects of mutating the polybasic region of septin 2, substituting basic residues with neutral ones. Indeed, as predicted, the mutant septin 2 failed to localize to membranes. Moreover, expression of the mutant septin 2 had a dominant negative effect, revealed by the loss of endogenous septin 2 from the membrane. The dominant negative effect is reasonable because septins form hetero-oligomers that assemble into filaments. The partial loss of the polybasic septin / acidic membrane lipid interaction is sufficient to cause the loss of septins from the membrane, consistent with additive interactions being necessary for association.

TNF-α and Septins

As part of the process of inflammation, the cytokine TNF-α causes increased permeability of the endothelium with partial loss of cell junction integrity[20]. We asked whether septin 2, based on its role in cell junction integrity, might be a component of the mechanism of action of TNF-α[55,79]. Indeed, we found that TNF-α treatment of endothelial monolayers causes loss of septin 2 filaments normally enriched at cell junctions, with shifting of their distribution to the cytoplasm. This change in septin 2 distribution appears to contribute to or perhaps be sufficient for the disorganization of junctional proteins that results from TNF-α treatment.

In addition, one might speculate that the membrane tethering of septin 2 by anionic phospholipids is regulated by TNF-α induced signaling pathways. TNF-α has been shown to activate PLC γ, which catalyzes the hydrolysis of PIP_2 at the membrane into IP_3 and DAG[80]. Thus, TNF-α may induce decreases in PIP_2 levels at the plasma membrane. We find this speculative hypothesis interesting but see it as likely to be an oversimplification. Treatment with TNF-α has many effects on endothelial cells in addition to the effects on septin 2 localization. On that point, our gene expression analysis revealed many notable differences between septin 2 depletion and TNF-α treatment.

Potential Interactive Role for Actin Filaments

We noted loss of F-actin associated with cell junctions, as a result of septin 2 suppression, septin 2 PIP_2BM expression, and TNF-α treatment. Septin filament networks and actin filament networks are known to have functional interdependence[26–31]. Therefore, the role of septin filaments at cell junctions may involve cooperative interactions among cytosolic actin filaments and cell junction components.

Potential Role of Septin 2 in Endothelial Cell Growth and Division

Septin genes were initially found to play a critical role in cytokinesis in budding yeast[1], and several studies have demonstrated a role for septins at the kinetochore in mammalian cell systems[81–83]. In this work, we found that septin 2 suppression resulted in an increase in cell size compared to control cells. We found no evidence for cell death with septin 2 suppression, and we found that the number of cells in our cultures increased at a slower rate. These effects may reflect roles of septins in regulation of cell growth and division based on biological pathways operating at the DNA level[84], in addition to the role of septins as regulators of the organization of junctional proteins at cell junctions.

Summary

Our results are summarized in a schematic diagram in Figure 6, which illustrates intercellular adhesion proteins and septin 2 at junctions of endothelial monolayers. Under basal conditions, septin 2 is localized at junctions mediated by interaction between PIP_2 at the membrane and basic residues in septin 2. Cell junctions are associated with well-organized structures of intercellular adhesion proteins, such as VE-cadherin, nectin-2, afadin, PECAM-1, and ZO-1. Septin 2 is enriched at the positively curved areas of membrane (Fig. 6A). Loss of septin 2 at cell junctions, caused by suppression of septin 2, treatment with TNF-α, and loss of interaction with membrane PIP_2 causes significant

alteration of the arrangement of junctional proteins and defects in the integrity of the barrier formed by endothelial monolayers (Fig. 6B).

Supplementary Material

Refer to Web version on PubMed Central for supplementary material.

Acknowledgements

We are extremely grateful to Olivia L. Mooren and Patrick McConnell for scoring the morphology of cell junctions as well as for advice and assistance. We are grateful to Michael D Onken for helping to score junction morphology and for invaluable advice related to statistical analysis and to RNA sequence experiments and data analysis. The Genome Technology Access Center (GTAC) of Washington University School of Medicine provided advice and assistance with RNA sequencing. Light microscopy was performed in part through the use of the Washington University Center for Cellular Imaging (WUCCI) supported by the Washington University School of Medicine, The Children's Discovery Institute of Washington University, and St. Louis Children's Hospital (CDI, CORE-2015–505) and NIH / NINDS NS086741.

Funding source

This work was funded by NIH R35 GM118171 to J.A.C.

Abbreviations

AJ	Adherens junction
F-actin	filamentous actin
HDMVECs	Human dermal microvascular endothelial cells
JAM	junctional adhesion molecule
PECAM-1	Platelet-endothelial cell adhesion molecule-1
PIP_2	Phosphatidylinositol 4,5-bisphosphate
TJ	Tight junction
TNF-α	Tumor necrosis factor alpha
VE	cadherin, Vascular endothelial-cadherin
ZO-1	Zonula occludens-1

References

1. Hartwell LH Genetic control of the cell division cycle in yeast. IV. Genes controlling bud emergence and cytokinesis. Exp Cell Res. 1971;69:265–276. [PubMed: 4950437]
2. Haarer BK & Pringle JR Immunofluorescence localization of the *Saccharomyces cerevisiae CDC12* gene product to the vicinity of the 10-nm filaments in the mother-bud neck. Mol. Cell. Biol 1987;7:3678–3687. [PubMed: 3316985]
3. Ong K, Wloka C, Okada S, Svitkina T & Bi E Architecture and dynamic remodelling of the septin cytoskeleton during the cell cycle. Nat Commun. 2014;5:5698. [PubMed: 25474997]
4. Oh Y & Bi E Septin structure and function in yeast and beyond. Trends Cell Biol. 2011;21:141–148. [PubMed: 21177106]

5. Mostowy S & Cossart P Septins: the fourth component of the cytoskeleton. Nat. Rev. Mol. Cell Biol 2012;13:183–194. [PubMed: 22314400]
6. Dolat L, Hu Q & Spiliotis ET Septin functions in organ system physiology and pathology. Biol. Chem 2014;395:123–141. [PubMed: 24114910]
7. Kinoshita M Assembly of mammalian septins. J. Biochem 2003;134:491–496. [PubMed: 14607974]
8. Pan F, Malmberg RL & Momany M Analysis of septins across kingdoms reveals orthology and new motifs. BMC Evol Biol. 2007;7:103. [PubMed: 17601340]
9. Cao L et al. Phylogenetic and evolutionary analysis of the septin protein family in metazoan. FEBS Lett. 2007;581:5526–5532. [PubMed: 17967425]
10. Bridges AA & Gladfelter AS Septin Form and Function at the Cell Cortex. J. Biol. Chem 2015;290:17173–17180. [PubMed: 25957401]
11. Valadares NF, d' Muniz Pereira H, Ulian Araujo AP & Garratt RC Septin structure and filament assembly. Biophys Rev. 2017;9:481–500. [PubMed: 28905266]
12. Zhang J et al. Phosphatidylinositol polyphosphate binding to the mammalian septin H5 is modulated by GTP. Curr. Biol 1999;9:1458–1467. [PubMed: 10607590]
13. Omrane M et al. Septin 9 has Two Polybasic Domains Critical to Septin Filament Assembly and Golgi Integrity. iScience. 2019;13:138–153. [PubMed: 30831549]
14. Bridges AA et al. Septin assemblies form by diffusion-driven annealing on membranes. Proc. Natl. Acad. Sci. U S A 2014;111:2146–2151. [PubMed: 24469790]
15. Bertin A et al. Three-dimensional ultrastructure of the septin filament network in *Saccharomyces cerevisiae*. Mol. Biol. Cell 2012;23:423–432. [PubMed: 22160597]
16. Rodal AA, Kozubowski L, Goode BL, Drubin DG & Hartwig JH Actin and septin ultrastructures at the budding yeast cell cortex. Mol. Biol. Cell 2005;16:372–384. [PubMed: 15525671]
17. Spiliotis ET & Gladfelter AS Spatial guidance of cell asymmetry: septin GTPases show the way. Traffic. 2012;13:195–203. [PubMed: 21883761]
18. Bridges AA, Jentzsch MS, Oakes PW, Occhipinti P & Gladfelter AS Micron-scale plasma membrane curvature is recognized by the septin cytoskeleton. J. Cell Biol 2016;213:23–32. [PubMed: 27044896]
19. Kang H & Lew DJ How do cells know what shape they are? Curr. Genet 2017;63:75–77. [PubMed: 27313005]
20. Kim J & Cooper JA Septins regulate junctional integrity of endothelial monolayers. Mol. Biol. Cell 2018;29:1693–1703. [PubMed: 29771630]
21. Dolat L et al. Septins promote stress fiber-mediated maturation of focal adhesions and renal epithelial motility. J. Cell Biol 2014;207:225–235. [PubMed: 25349260]
22. Fung KY, Dai L & Trimble WS Cell and molecular biology of septins. Int Rev Cell Mol Biol. 2014;310:289–339. [PubMed: 24725429]
23. Spiliotis ET & Nelson WJ Here come the septins: novel polymers that coordinate intracellular functions and organization. J. Cell Sci 2006;119:4–10. [PubMed: 16371649]
24. Pagliuso A et al. A role for septin 2 in Drp1-mediated mitochondrial fission. EMBO Rep. 2016;17:858–873. [PubMed: 27215606]
25. Dolat L & Spiliotis ET Septins promote macropinosome maturation and traffic to the lysosome by facilitating membrane fusion. J. Cell Biol 2016;214:517–527. [PubMed: 27551056]
26. Bezanilla M, Gladfelter AS, Kovar DR & Lee WL Cytoskeletal dynamics: a view from the membrane. J. Cell Biol 2015;209:329–337. [PubMed: 25963816]
27. Hu J et al. Septin-driven coordination of actin and microtubule remodeling regulates the collateral branching of axons. Curr. Biol 2012;22:1109–1115. [PubMed: 22608511]
28. Joo E, Surka MC & Trimble WS Mammalian SEPT2 is required for scaffolding nonmuscle myosin II and its kinases. Dev Cell. 2007;13:677–690. [PubMed: 17981136]
29. Mavrakis M et al. Septins promote F-actin ring formation by crosslinking actin filaments into curved bundles. Nat. Cell Biol 2014;16:322–334. [PubMed: 24633326]
30. Spiliotis ET Spatial effects - site-specific regulation of actin and microtubule organization by septin GTPases. J. Cell Sci 2018;131

31. Spiliotis ET, Hunt SJ, Hu Q, Kinoshita M & Nelson WJ Epithelial polarity requires septin coupling of vesicle transport to polyglutamylated microtubules. J. Cell Biol 2008;180:295–303. [PubMed: 18209106]
32. Baldwin AL & Thurston G Mechanics of endothelial cell architecture and vascular permeability. Crit Rev Biomed Eng. 2001;29:247–278. [PubMed: 11417757]
33. Deanfield JE, Halcox JP & Rabelink TJ Endothelial function and dysfunction: testing and clinical relevance. Circulation. 2007;115:1285–1295. [PubMed: 17353456]
34. Michiels C Endothelial cell functions. J. Cell. Physiol 2003;196:430–443. [PubMed: 12891700]
35. Sumpio BE, Riley JT & Dardik A Cells in focus: endothelial cell. Int J Biochem Cell Biol. 2002;34:1508–1512. [PubMed: 12379270]
36. Bazzoni G & Dejana E Endothelial cell-to-cell junctions: molecular organization and role in vascular homeostasis. Physiol. Rev 2004;84:869–901. [PubMed: 15269339]
37. Dejana E Endothelial cell-cell junctions: happy together. Nat. Rev. Mol. Cell Biol 2004;5:261–270. [PubMed: 15071551]
38. Lampugnani MG, Dejana E & Giampietro C Vascular Endothelial (VE)-Cadherin, Endothelial Adherens Junctions, and Vascular Disease. Cold Spring Harb Perspect Biol. 2017 doi: 10.1101/cshperspect.a029322.
39. Giannotta M, Trani M & Dejana E VE-cadherin and endothelial adherens junctions: active guardians of vascular integrity. Dev Cell. 2013;26:441–454. [PubMed: 24044891]
40. Sakakibara S, Maruo T, Miyata M, Mizutani K & Takai Y Requirement of the F-actin-binding activity of l-afadin for enhancing the formation of adherens and tight junctions. Genes Cells. 2018;23:185–199. [PubMed: 29431241]
41. Tabariès S et al. Afadin cooperates with Claudin-2 to promote breast cancer metastasis. Genes Dev. 2019;33:180–193. [PubMed: 30692208]
42. Heinemann U & Schuetz A Structural Features of Tight-Junction Proteins. Int J Mol Sci. 2019;20
43. Buckley A & Turner JR Cell Biology of Tight Junction Barrier Regulation and Mucosal Disease. Cold Spring Harb Perspect Biol. 2018;10
44. McNeil E, Capaldo CT & Macara IG Zonula occludens-1 function in the assembly of tight junctions in Madin-Darby canine kidney epithelial cells. Mol. Biol. Cell 2006;17:1922–1932. [PubMed: 16436508]
45. Tornavaca O et al. ZO-1 controls endothelial adherens junctions, cell-cell tension, angiogenesis, and barrier formation. J. Cell Biol 2015;208:821–838. [PubMed: 25753039]
46. Ebnet K, Suzuki A, Ohno S & Vestweber D Junctional adhesion molecules (JAMs): more molecules with dual functions. J. Cell Sci 2004;117:19–29. [PubMed: 14657270]
47. Kumar NM & Gilula NB The gap junction communication channel. Cell. 1996;84:381–388. [PubMed: 8608591]
48. Saez JC, Berthoud VM, Branes MC, Martinez AD & Beyer EC Plasma membrane channels formed by connexins: their regulation and functions. Physiol. Rev 2003;83:1359–1400. [PubMed: 14506308]
49. Privratsky JR & Newman PJ PECAM-1: regulator of endothelial junctional integrity. Cell Tissue Res. 2014;355:607–619. [PubMed: 24435645]
50. Hahn JH et al. CD99 (MIC2) regulates the LFA-1/ICAM-1-mediated adhesion of lymphocytes, and its gene encodes both positive and negative regulators of cellular adhesion. J. Immunol 1997;159:2250–2258. [PubMed: 9278313]
51. Schenkel AR, Mamdouh Z, Chen X, Liebman RM & Muller WA CD99 plays a major role in the migration of monocytes through endothelial junctions. Nat. Immunol 2002;3:143–150. [PubMed: 11812991]
52. Hartsock A & Nelson WJ Adherens and tight junctions: structure, function and connections to the actin cytoskeleton. Biochim. Biophys. Acta 2008;1778:660–669. [PubMed: 17854762]
53. Garcia-Ponce A, Citalán-Madrid AF, Velázquez-Avila M, Vargas-Robles H & Schnoor M The role of actin-binding proteins in the control of endothelial barrier integrity. Thromb. Haemost 2015;113:20–36. [PubMed: 25183310]

54. Mooren OL, Kim J, Li J & Cooper JA Role of N-WASP in Endothelial Monolayer Formation and Integrity. J. Biol. Chem 2015;290:18796–18805. [PubMed: 26070569]
55. Mooren OL, Li J, Nawas J & Cooper JA Endothelial cells use dynamic actin to facilitate lymphocyte transendothelial migration and maintain the monolayer barrier. Mol. Biol. Cell 2014;25:4115–4129. [PubMed: 25355948]
56. Schnittler H et al. Actin filament dynamics and endothelial cell junctions: the Ying and Yang between stabilization and motion. Cell Tissue Res. 2014;355:529–543. [PubMed: 24643678]
57. Mooren OL, Kotova TI, Moore AJ & Schafer DA Dynamin2 GTPase and cortactin remodel actin filaments. J. Biol. Chem 2009;284:23995–24005. [PubMed: 19605363]
58. Schindelin J et al. Fiji: an open-source platform for biological-image analysis. Nat Methods. 2012;9:676–682. [PubMed: 22743772]
59. Dobin A et al. STAR: ultrafast universal RNA-seq aligner. Bioinformatics. 2013;29:15–21. [PubMed: 23104886]
60. Liao Y, Smyth GK & Shi W featureCounts: an efficient general purpose program for assigning sequence reads to genomic features. Bioinformatics. 2014;30:923–930. [PubMed: 24227677]
61. Patro R, Duggal G, Love MI, Irizarry RA & Kingsford C Salmon provides fast and bias-aware quantification of transcript expression. Nat Methods. 2017;14:417–419. [PubMed: 28263959]
62. Wang L, Wang S & Li W RSeQC: quality control of RNA-seq experiments. Bioinformatics. 2012;28:2184–2185. [PubMed: 22743226]
63. Robinson MD, McCarthy DJ & Smyth GK edgeR: a Bioconductor package for differential expression analysis of digital gene expression data. Bioinformatics. 2010;26:139–140. [PubMed: 19910308]
64. Ritchie ME et al. limma powers differential expression analyses for RNA-sequencing and microarray studies. Nucleic Acids Res. 2015;43:e47. [PubMed: 25605792]
65. Liu R et al. Why weight? Modelling sample and observational level variability improves power in RNA-seq analyses. Nucleic Acids Res. 2015;43:e97. [PubMed: 25925576]
66. Cerutti C & Ridley AJ Endothelial cell-cell adhesion and signaling. Exp Cell Res. 2017;358:31–38. [PubMed: 28602626]
67. Tanaka-Takiguchi Y, Kinoshita M & Takiguchi K Septin-mediated uniform bracing of phospholipid membranes. Curr. Biol 2009;19:140–145. [PubMed: 19167227]
68. Bertin A et al. Phosphatidylinositol-4,5-bisphosphate promotes budding yeast septin filament assembly and organization. J. Mol. Biol 2010;404:711–731. [PubMed: 20951708]
69. Xie H, Surka M, Howard J & Trimble WS Characterization of the mammalian septin H5: distinct patterns of cytoskeletal and membrane association from other septin proteins. Cell Motil. Cytoskeleton 1999;43:52–62. [PubMed: 10340703]
70. Efimova N & Svitkina TM Branched actin networks push against each other at adherens junctions to maintain cell-cell adhesion. J. Cell Biol 2018;217:1827–1845. [PubMed: 29507127]
71. Takai Y & Nakanishi H Nectin and afadin: novel organizers of intercellular junctions. J. Cell Sci 2003;116:17–27. [PubMed: 12456712]
72. Mandai K et al. Afadin: A novel actin filament-binding protein with one PDZ domain localized at cadherin-based cell-to-cell adherens junction. J. Cell Biol 1997;139:517–528. [PubMed: 9334353]
73. Okumura N, Kagami T, Fujii K, Nakahara M & Koizumi N Involvement of Nectin-Afadin in the Adherens Junctions of the Corneal Endothelium. Cornea. 2018;37:633–640. [PubMed: 29384809]
74. Woodfin A, Voisin MB & Nourshargh S PECAM-1: a multi-functional molecule in inflammation and vascular biology. Arterioscler Thromb Vasc Biol. 2007;27:2514–2523. [PubMed: 17872453]
75. Zhang J et al. Phosphatidylinositol polyphosphate binding to the mammalian septin H5 is modulated by GTP. Curr. Biol 1999;9:1458–1467. [PubMed: 10607590]
76. Cannon KS, Woods BL, Crutchley JM & Gladfelter AS An amphipathic helix enables septins to sense micrometer-scale membrane curvature. J. Cell Biol 2019;218:1128–1137. [PubMed: 30659102]
77. Beber A et al. Membrane reshaping by micrometric curvature sensitive septin filaments. Nat Commun. 2019;10:420. [PubMed: 30679428]

78. McLaughlin S, Wang J, Gambhir A & Murray D PIP(2) and proteins: interactions, organization, and information flow. Annu Rev Biophys Biomol Struct. 2002;31:151–175. [PubMed: 11988466]

79. Goldblum SE, Hennig B, Jay M, Yoneda K & McClain CJ Tumor necrosis factor alpha-induced pulmonary vascular endothelial injury. Infect. Immun 1989;57:1218–1226. [PubMed: 2925247]

80. Chen CC, Sun YT, Chen JJ & Chiu KT TNF-alpha-induced cyclooxygenase-2 expression in human lung epithelial cells: involvement of the phospholipase C-gamma 2, protein kinase C-alpha, tyrosine kinase, NF-kappa B-inducing kinase, and I-kappa B kinase 1/2 pathway. J. Immunol 2000;165:2719–2728. [PubMed: 10946303]

81. Zhu M et al. Septin 7 interacts with centromere-associated protein E and is required for its kinetochore localization. J. Biol. Chem 2008;283:18916–18925. [PubMed: 18460473]

82. Thomas S & Kaplan KB A Bir1p Sli15p kinetochore passenger complex regulates septin organization during anaphase. Mol. Biol. Cell 2007;18:3820–3834. [PubMed: 17652458]

83. Gillis AN, Thomas S, Hansen SD & Kaplan KB A novel role for the CBF3 kinetochore-scaffold complex in regulating septin dynamics and cytokinesis. J. Cell Biol 2005;171:773–784. [PubMed: 16330709]

84. Veitia RA DNA Content, Cell Size, and Cell Senescence. Trends Biochem. Sci 2019;44:645–647. [PubMed: 31160123]

Highlights

- Loss of Septin 2 at cell junctions of a microvascular endothelial monolayer leads to disorganization of adherens junction components (nectin-2 and afadin), the tight junction component ZO-1, and the cell adhesion molecule PECAM-1.
- Inflammatory cytokine TNF-α induces loss of septin 2 at cell junctions.
- Junctional localization of septin 2 is mediated by interaction of the polybasic domain of septin 2 with acidic phospholipids in the plasma membrane.
- RNA sequence data shows numerous genes with significant changes in expression in response to septin 2 suppression and to TNF-α treatment in human microvascular endothelial cells.

Hightlights

- Under basal conditions, septin 2 is localized at junctions mediated by interaction between PIP_2 at the membrane and basic residues in septin 2.
- Cell junctions are associated with well-organized structures of intercellular adhesion proteins, such as VE-cadherin, nectin-2, afadin, PECAM-1, and ZO-1. Septin 2 is enriched at the positively curved areas of membrane.
- Loss of septin 2 at cell junctions, caused by suppression of septin 2, treatment with TNF-α, and loss of interaction with membrane PIP_2 causes significant alteration of the arrangement of junctional proteins and defects in the integrity of the barrier formed by endothelial monolayers.

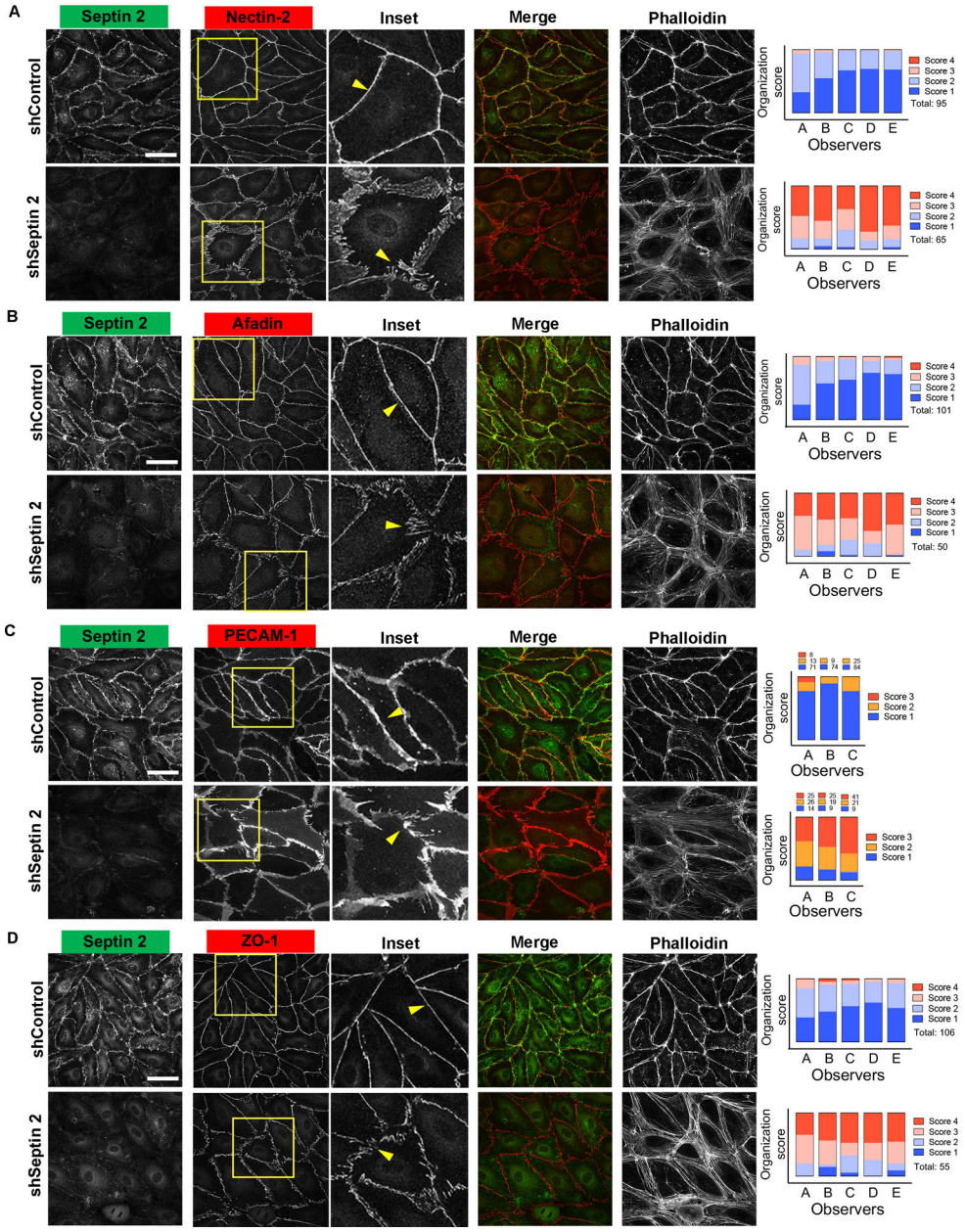

Figure 1. Suppression of septin 2 protein results in the disorganization of junctional proteins.

Immunofluorescence staining for endogenous septin 2 (green), cell-cell adhesion proteins (red), and actin filaments in HDMVECs and scoring of the organization of junctional molecules (A-D). Inset shows the enlarged area of cell-cell adhesion molecules. (A) Endogenous septin 2, nectin-2, actin filaments, and blind scores of nectin-2 organization are shown in control (Upper) and septin 2-suppressed HDMVECs (Lower). (B) Endogenous septin 2, afadin, actin filaments, and blind scores of afadin organization are shown in control (Upper) and septin 2-suppressed HDMVECs (Lower). (C) Endogenous septin 2, PECAM-1, actin filaments, and blind scores of PECAM-1 organization are shown in control (Upper) and septin 2-suppressed HDMVECs (Lower). (D) Endogenous septin 2, tight junction protein (ZO-1), actin filaments, and blind scores of ZO-1 organization are shown in control

(Upper) and septin 2-suppressed HDMVECs (Lower). Scale bars: 50 μm. Variances among observers are statistically not significant. Differences in the organization of junctional proteins between control and septin 2-suppressed HDMVECs are statistically significant. p-values are < 0.0001.

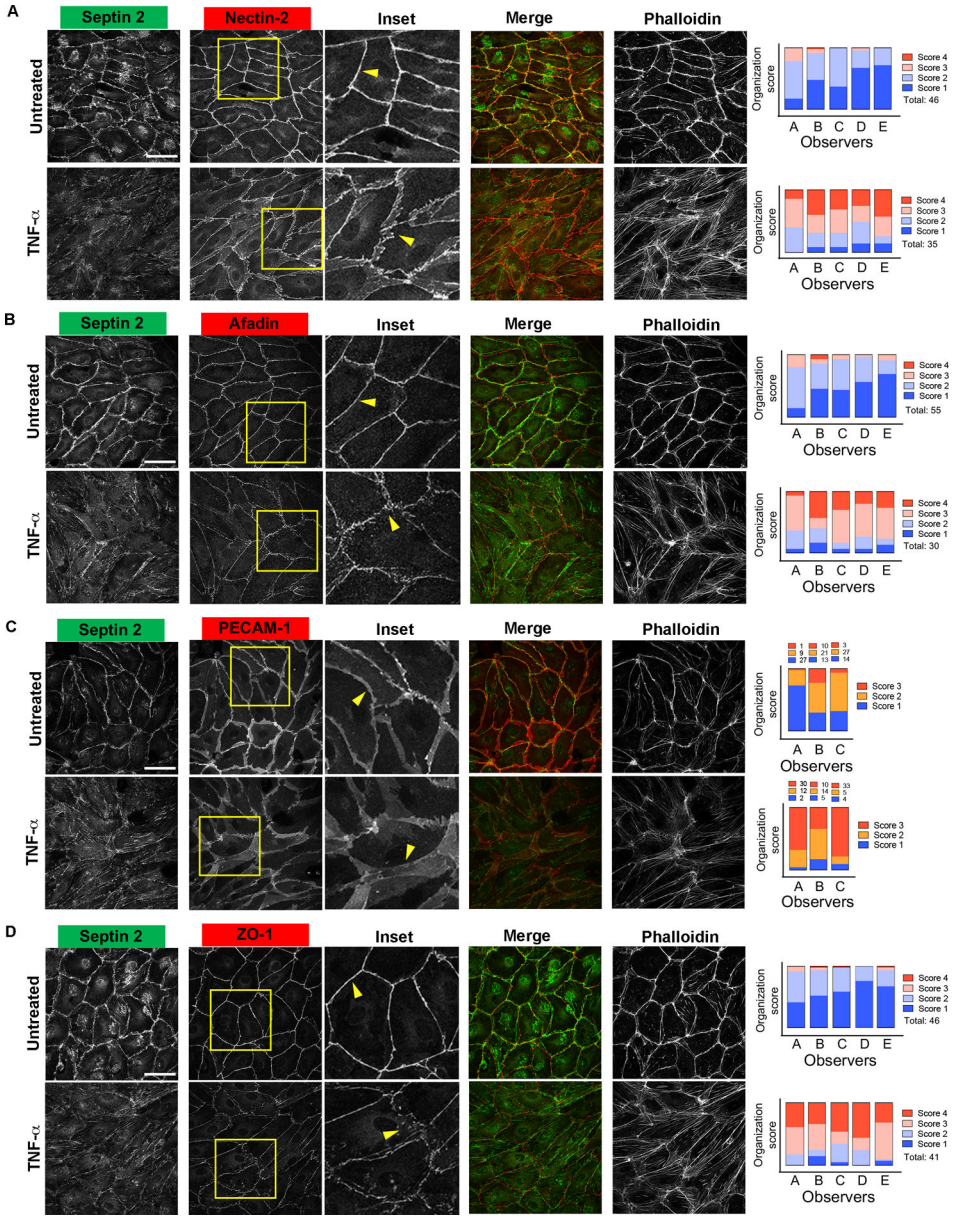

Figure 2. TNF-α treatment sequesters septin 2 to the cytoplasm in association with the disorganization of junctional proteins.

Immunofluorescence staining for endogenous septin 2 (green), cell-cell adhesion proteins (red) and actin filaments in HDMVECS and scoring of the organization of junctional molecules (A-D). Insets indicate enlarged area of the image. (A) Endogenous septin 2, nectin-2, actin filaments, and blind scores of nectin-2 organization are shown in untreated (Upper) and TNF-α-treated HDMVECs (Lower). (B) Endogenous septin 2, afadin, actin filaments, and blind scores of afadin organization are shown in untreated (Upper) and TNF-α-treated HDMVECs (Lower). (C) Endogenous septin 2, PECAM-1, actin filaments, and blind scores of PECAM-1 organization are shown in untreated (Upper) and TNF-α-treated HDMVECs (Lower). (D) Endogenous septin 2, ZO-1, actin filaments, and blind scores of ZO-1 organization are shown in untreated (Upper) and TNF-α-treated HDMVECs (Lower).

Scale bars: 50 μm. Variances among observers are statistically not significant. Differences in the organization of junctional proteins between untreated and TNF-α-treated HDMVECs are statistically significant. p-values are < 0.0001.

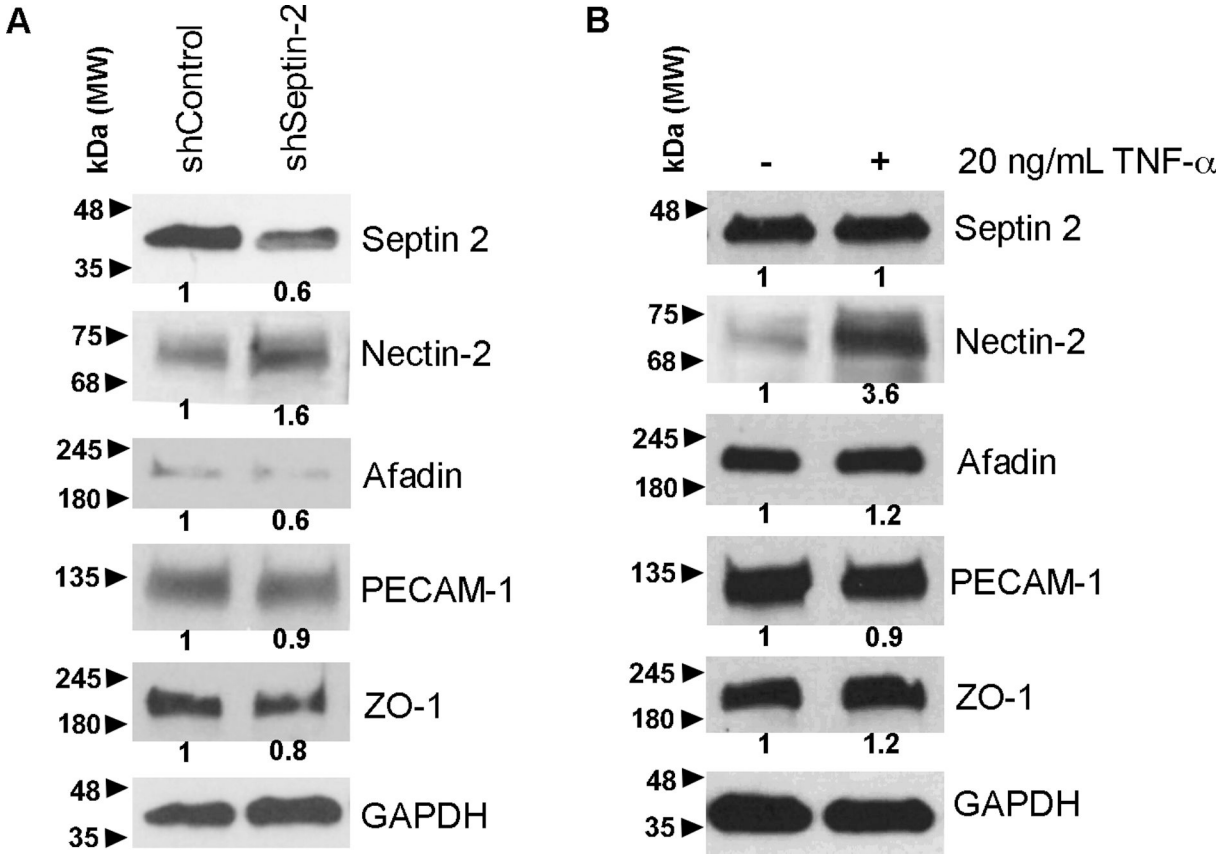

Figure 3. Expression levels of intercellular adhesion proteins in response to septin 2 suppression and TNF-α treatment.

Immunoblot analysis for junctional adhesion proteins. Expression levels of each protein are shown in response to (A) septin 2 suppression and (B) TNF-α treatment. GAPDH is an internal loading control. Band intensities acquired using ImageJ are shown.

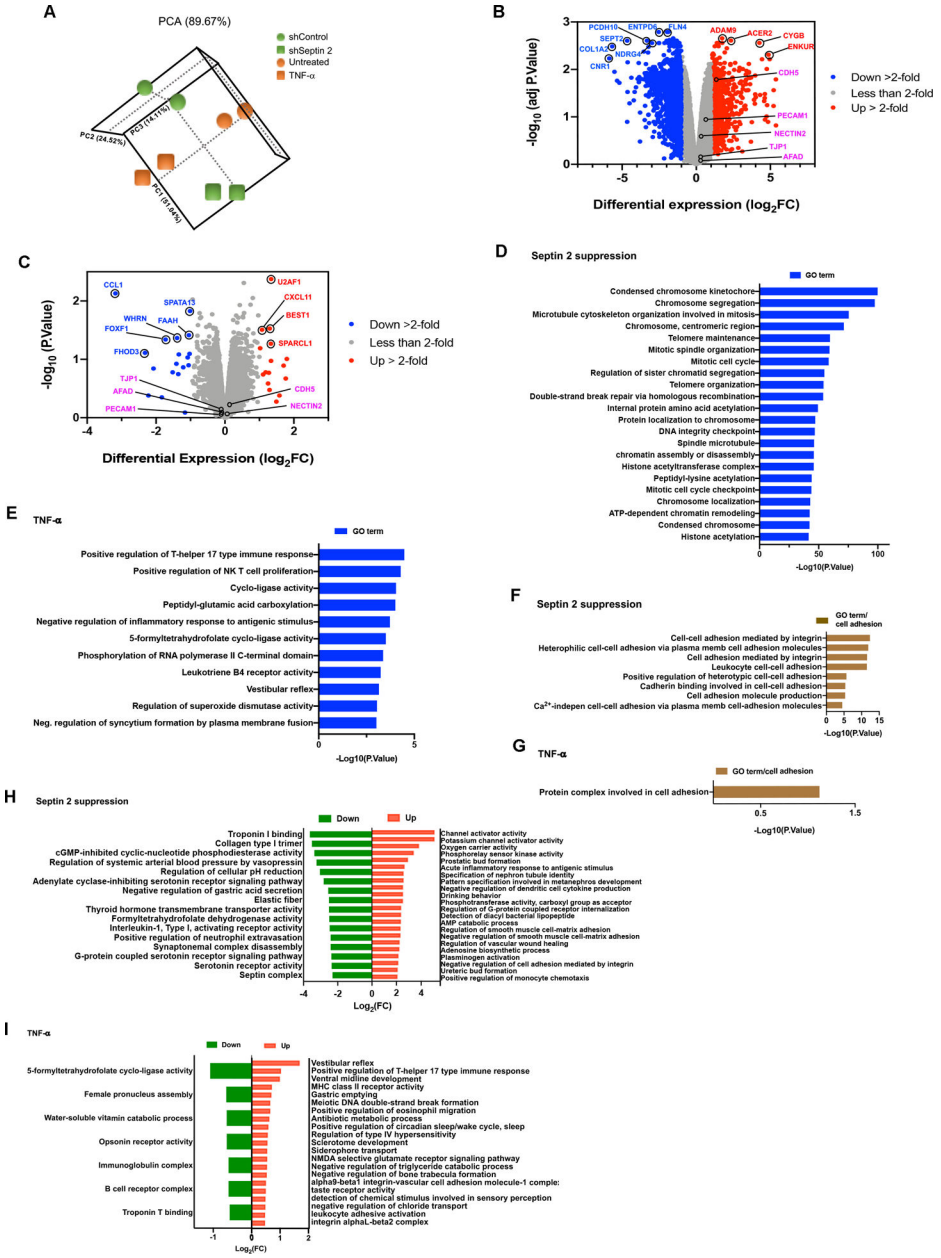

Figure 4. RNA sequence analysis with HDMVECs in response to septin 2 suppression and TNF-α treatment.

(A) Principal component analysis (PCA) of septin 2-suppressed and TNF-α-treated HDMVECs. PCA was performed with all genes. (B) Volcano plot of septin 2 suppression compared to control highlights differentially expressed genes using a fold-change > 2 as the cut-off value. (C) Volcano plot of TNF-α treatment compared to no treatment highlights differentially expressed genes using a fold-change > 2 as the cut-off value. Selected over-represented GO terms associated with various biological processes (D-E), cell-cell adhesion processes (F-G) and absolute fold-change > or <2 (H-l). Septin 2 suppression is compared to control, and TNF-α treatment is compared to no treatment.

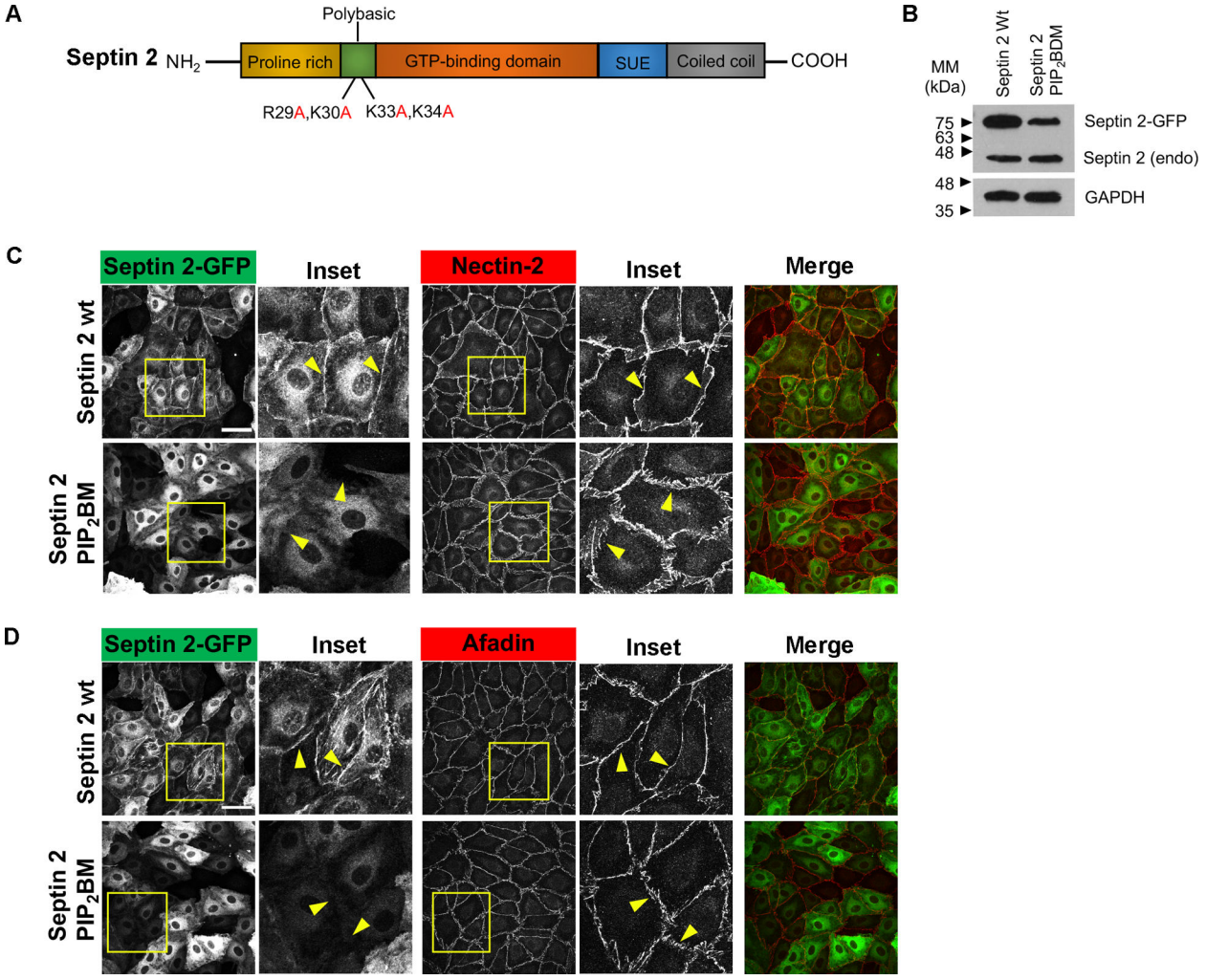

Figure 5. Polybasic mutant septin 2 fails to localize to cell junctions.

(A) Diagram of septin 2 domain architecture shows four basic residues, R and K, in the polybasic domain at the N-terminus. (B) Ectopic overexpression levels of septin 2 wild type (wt)-GFP and septin 2 PIP_2 binding mutant (BM)-GFP. (C-D) Immunofluorescence staining shows overexpression of septin 2 wt and PIP_2 BM (green), junctional proteins (red), and actin filaments. (C) Overexpression of septin 2 wt-GFP and septin 2 PIP_2BM-GFP (Upper, Inset) and organization of nectin-2 at cell junctions (Lower, Inset). (D) Overexpression of septin 2 wt-GFP and septin 2 PIP_2BM-GFP (Upper, Inset) and organization of afadin at cell junctions (Lower, Inset). Scale bars: 50 μm

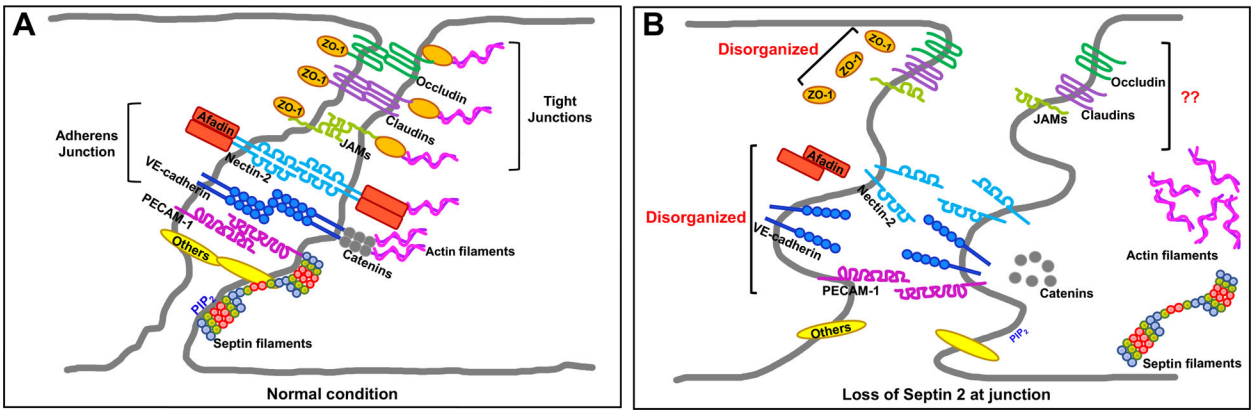

Figure 6. Diagram of septin 2 and intercellular junctional proteins at endothelial cell junctions.

(A) Under control resting conditions, septin 2 filaments are localized at junctions of microvascular endothelial cells, and various junctional proteins are properly organized at cell junctions. (B) Loss of septin 2 at cell junctions leads to the disorganization of junctional components of microvascular endothelial monolayers resulting in loss of junctional integrity.